A Journal of the Gesellschaft Deutscher Chemiker

Angewandte International Edition GDCh Chemie

www.angewandte.org

Accepted Article

Title: Palladium-Catalyzed Enantioselective Migratory Hydroamidocarbonylation of Amide-Linked Alkenes to Access Chiral α-Alkyl Succinimides

Authors: Zhen Wang, Chaoren Shen, and Kaiwu Dong

To be cited as: *Angew. Chem. Int. Ed.* **2024**, e202410967

Link to VoR: https://doi.org/10.1002/anie.202410967

WILEY VCH

10.1002/anie.202410967

WILEY-VCH

RESEARCH ARTICLE

Palladium-Catalyzed Enantioselective Migratory Hydroamidocarbonylation of Amide-Linked Alkenes to Access Chiral α-Alkyl Succinimides

Zhen Wang,[a] Chaoren Shen[a] and Kaiwu Dong*[a,b]

[a] Shanghai Key Laboratory of Green Chemistry and Chemical Processes, State Key Laboratory of Petroleum Molecular & Process Engineering, School of Chemistry and Molecular Engineering, East China Normal University, Shanghai 200062, China

[b] Shanghai Frontiers Science Center of Molecule Intelligent Syntheses, School of Chemistry and Molecular Engineering, East China Normal University, Shanghai 200062, China

E-mail: kwdong@chem.ecnu.edu.cn

Supporting information for this article is given via a link at the end of the document.

Abstract: A Pd-catalyzed asymmetric isomerization-hydroamidocarbonylation of amide-containing alkenes was developed, affording a variety of chiral α-alkyl succinimides in moderate to good yields with high enantioselectivities. The key to success was introducing bulky 1-adamentyl *P*-substitution and 2,3,5,6-tetramethoxyphenyl group into the rigid *P*-chirogenic bisphosphine ligand to create stronger steric hinderance and deeper catalytic pocket. By this approach, regio- or stereo-convergent synthesis of enantiomeric succinimides from the mixture of olefin isomers was achieved.

Introduction

Catalytic enantioselective hydrofunctionalization of alkenes provides a straightforward approach to chiral molecules,[1-8] while integration of alkene isomerization and stereoselective hydrofunctionalization may achieve remote asymmetric C(sp^3)−H functionalization[9-12] and implement convergent transformation of isomeric olefin mixture to single enantiomer. Whereas both alkene isomerization[13] and asymmetric hydrofunctionalization may involve the use of a transition-metal hydride catalyst, development of an efficient catalyst system that can accomplish the two transformation in a single process is challenging but highly desirable. In this context, most of the reported asymmetric isomerization-hydrofunctionalization progresses so far are based on the use of in-situ formed chiral nickel-hydride species (Figure 1a).[14-19] On the other hand, the application of palladium catalysts in such a cascade process is less explored, despite of their versatile uses in alkene hydrofunctionalization.[20] Recently, Pd-catalyzed enantioselective migratory hydroalkylation of skipped or conjugated dienes with active methylene compounds was disclosed (Figure 1a),[21] suggesting a good potential in the development of Pd-catalyzed enantioselective conversion of isomeric alkene mixtures to chiral functionalized molecules.

Enantioselective hydrocarboxylation of alkenes with CO and nucleophiles is considered as a straightforward route to synthesize chiral carboxylic acids and their derivatives.[22] In this context, the catalytic hydrocarboxylation of internal alkenes to linear esters has been well established,[23-26] whereas transition metal catalyzed regio- and enantioselective migratory hydrocarboxylation of terminal alkenes to branched or cyclic products still remains elusive so far. The non-asymmetric isomerization-hydroamidocarbonylation of terminal alkenes bearing an internal amido group occurring at an internal C(sp^3)-H site has been reported by using a tungsten carbonyl catalyst (Figure 1b).[27] In this case, the stereogenic center of the product is forged at the carbon atom adjacent to the carbonyl group, hence the enantioselectivity would be affected by the spatial environment surrounding metal center. Moreover, previous studies have shown that the enantioselectivity of hydrocarbonylation is usually determined in the step of either Pd-H addition onto alkene or alcoholysis of Pd-acyl intermediate.[28] Thus, we conceived that creating a more congested chiral spatial environment around Pd center by introducing bulky substituents to the ligand[29] might be beneficial for the enantioselectivity control. We envisioned that modification of a Pd catalyst with *P*-chirogenic phosphine ligand featured by geometric rigidity[30] might enable both chain-walking mechanism[31] for terminal alkene isomerization and subsequent enantioselective hydrocarboxylation. Herein, by using a bulky chiral diphosphine ligand that bears 2,3-dihydrobenzo[*d*][1,3]oxaphosphole motif,[32] an unprecedented Pd-catalyzed regio- and enantioselective migratory hydroamidocarbonylation of alkenes was developed (Figure 1c). A diversity of chiral succinimide derivatives were synthesized in moderate to high yields with high enantioselectivities. The possible effects of the ligand on catalytic activity and enantioselectivity was rationalized by combined experimental and computational investigations.

10.1002/anie.202410967

WILEY VCH

RESEARCH ARTICLE

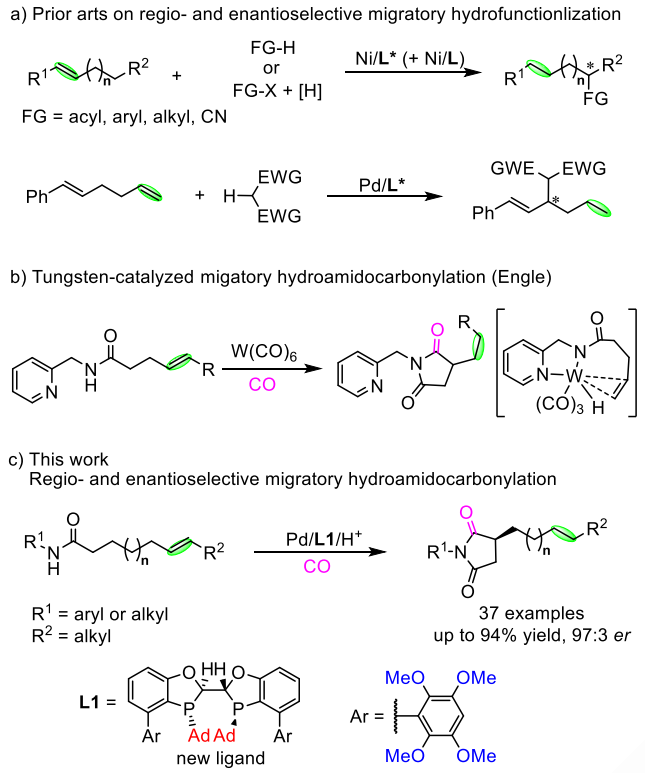

Figure 1. Regio- and/or enantioselective migratory hydrofunctionalization.

Results and Discussion

Initially, a series of *P*-chirogenic phosphine ligands bearing bulky 1-adamantyl *P*-substitution and different aryl substituents on the 4,4'-poistion of rigid 2,3-dihydrobenzo[*d*][1,3]oxaphosphole skeleton (**L1**-**L4**) were prepared. The regio- and enantioselective migratory hydroamidocarbonylation was investigated using olefin **1a** bearing an amide group as the model substrate, and *P*-adamantyl-substituted ligands (**L1**-**L4**) as well as *P*-*tert*-butyl-substitution analogs (**L5**-**L8**) were surveyed in the reaction. The reactions were typically run in xylenes at 80 °C under 30 bar pressure of CO, and the results were summarized in Table 1. The results disclosed that the enantioselectivity was effectively improved by switching the *P*-substitution from *tert*-butyl to bulkier 1-adamantyl group (entries 1-4 *vs.* 5-8, respectively). Within the groups of the *P*-chirogenic ligands bearing an 1-adamantyl group, higher yield of **2a** was obtained in the reactions catalyzed by ligands **L1** and **L2**, bearing 2,3,5,6-tetramethoxy- or 2,6-dimethoxy-substitued phenyl rings, respectively, on the 4,4'-positions of the 2,3-dihydrobenzo[*d*][1,3]oxaphosphole backbone (entries 1 and 2 *vs.* entries 3 and 4). Variations in other reaction conditions were also evaluated (Table 1, entries 9-14). While reducing the pressure of CO or the temperature led to a diminished yield of product **2a** (entries 9 and 10), elevating the temperature to 100 °C enhanced the yield albeit at the cost of a decreased enantiomeric ratio (*er*) (entry 11). Decreasing the loading of Pd catalyst or acid promoter resulted in a decline of yield (entries 12 and 13). Replacing xylenes with toluene as solvent slightly reduced the yield and enantioselectivity (entry 14). When 2 equiv. of MeOH was introduced into the reaction system, the reaction pathway was switched to methoxycarbonylation, affording the corresponding linear ester as the major byproduct (entry 15). After dearylation by oxidative C-N bond cleavage, **2a** was converted to enantiomeric 2-ethylsuccinimide in good yield (Section 5 in SI). By comparing the specific rotation of chiral 2-ethylsuccinimide with the literature,[33] the absolute configuration of **2a** was determined as (*S*)-configuration.

Table 1. Optimization of reaction conditions.[a]

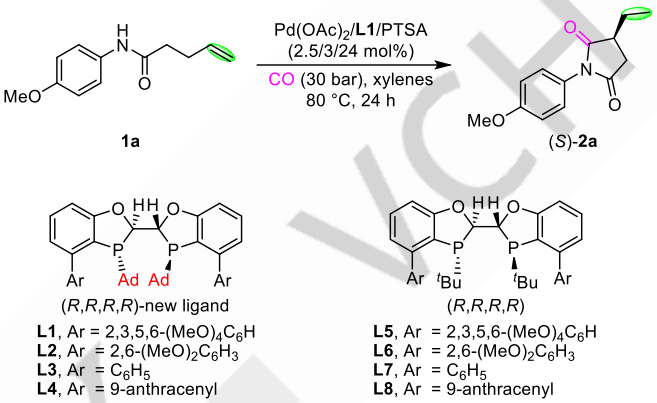

entry	variation from the standard conditions	yield (%)	*er*
1	None	87 (85)	95.5:4.5
2	**L2** instead of **L1**	89 (86)	94.5:5.5
3	**L3** instead of **L1**	56	78.5:21.5
4	**L4** instead of **L1**	51	89.5:10.5
5	**L5** instead of **L1**	84	92:8
6	**L6** instead of **L1**	70	88.5:11.5
7	**L7** instead of **L1**	88	73.5:26.5
8	**L8** instead of **L1**	89	84.5:15.5
9	15 bar instead of 30 bar CO	78	95:5
10	60 °C instead of 80 °C	46	95.5:4.5
11	100 °C instead of 80 °C	94	94:6
12	1 mol% Pd instead of 2.5 mol%	55	95:5
13	12 mol% PTSA instead of 24 mol%	74	95.5:4.5
14	toluene instead of xylenes	85	93:7
15	2.0 equiv. MeOH was added[b]	<5%	-/-

[a] Reaction conditions: **1a** (0.2 mmol), $Pd(OAc)_2$ (2.5 mol%), **L1** (5.6 mg, 3.0 mol%), PTSA (9.2 mg, 24 mol%), xylenes (1 mL), 30 bar CO, 80 °C, 24 h. Yield was determined by ^1H NMR using CH_2Br_2 as the internal standard after the reaction. In the parentheses were isolated yields. *Er* was determined by chiral HPLC. [b] Methyl 6-((4-methoxyphenyl)amino)-6-oxohexanoate was obtained in almost quantitative yield. PTSA = *p*-toluenesulfonic acid. Ad = 1-adamantyl.

With the optimized conditions in hand, the scope of amide-linked alkenes was explored (Scheme 1). For reactions of the terminal alkenes with a *N*-aryl amide, various electron-donating and -withdrawing substitutions on the phenyl ring were tolerated, affording the chiral succinimides **2b**-**2j** in good to high yields with excellent er values. Substrates containing a heteroaryl, 2-naphthyl, or a 3,4,5-trimethoxyphenyl substituent were compatible with the protocol, and the corresponding products **2k**-**2n** were obtained in good to high yields with good enantioselectivity. For reactions of terminal alkenes bearing a *N*-

10.1002/anie.202410967

alkyl amide, moderate to good yields of **2o** and **2p** with high *er* were achieved. Thienyl group was also compatible (**2q**). When chiral α-methyl benzyl amine (**2r**), phenyl alanine (**2s**), or α-amino ether (**2t**) was attached as the amide pendant, high diastereoselectivity was achieved. Moreover, alkenes containing dehydroabietic acid- or stilbene-derived amide group underwent the carbonylation smoothly, giving the product with high yield and selectivity (**2u** and **2v**).

This migratory hydroamidocarbonylation was applicable to 1,1-disubstituted terminal alkene, delivering the product **2w** in moderate yield and high enantioselectivity. The absolute configuration of **2w** was determined as (*R*) by X-ray crystallographic diffraction analysis.[34] Under the standard reaction conditions, migratory hydroamidocarbonylation of internal alkenes also achieved good regioselectivity and enantioselectivity (**2x**-**2aa**). Especially, the stereogenic center and the internal alkene double bond of the substrate derived from citronellal were retained (**2z**). The performance in the enantioselective isomerization-carbonylation of alkene bearing phenyl pendant (**2aa**) was well. The isomerization still preferred *β*,*γ*-position of amide group and the regioselectivity was unaffected. Encouraged by these results, we tested the reactions of the terminal alkenes with a longer aliphatic chain tethered to the amide functionality. Gratifyingly, the tandem isomerization-carbonylation proceeded smoothly and moderate yields of the corresponding products **2ab**-**2af** were obtained with good enantioselectivity. Even after isomerization over five positions, the hydroamidocarbonylation can still reach moderate yield with good *er* (**2af**). Last but not least, the protocol can be applied to biomass-based alkenes. This catalytic system exhibited good activity and selectivity in the enantioselective isomerization-carbonylation of oleic and elaidic acid-based alkenes (**2ah**).

We have also examined the use of this catalytic system in application of isomeric alkene mixtures (Scheme 2). Hydroamidocarbonylation using the mixture of regio-isomers **1ae** and **1ag** was found to proceed in a regio-convergent manner to deliver the product **2ad** in 80% yield with good enantioselectivity. Stereo-convergent hydroamidocarbonylation of the mixture of stereo-isomers (*Z*)- and (*E*)-**1ah** produced **2ah** in good yield and enantioselectivity. With the alkyne methoxycarbonylation[35] followed by amidation, 1-pentyne, 1-hexyne and 1-octyne could be converted to the mixtures of α,β-unsaturated and double-bond isomerized amides, respectively (**1ai**, **1aj**, **1ak**). These alkene mixtures could be transformed to the corresponding enantiomeric succinimides by this enantioselective isomerizing hydroamidocarbonylation. These results further demonstrated the remarkable utility of this catalytic system transforming regio- or stereo-isomeric alkene mixtures to chiral carboxylic acid derivatives.

The synthetic versatility of the succinimide products was showcased in several synthetic derivations of **2a**. For examples, 3-ethyl pyrrolidine **3a**, α-ethyl δ-valerolactam **4a**, α-ethyl-γ-nitrile δ-valerolactam **5a**, or compound **6a** was obtained by double amide reduction, chemoselective amide reduction, amide reduction-nucleophilic substitution, or dearylation, which showed the diverse utility of this migratory hydroamidocarbonylation in the synthesis of chiral *N*-heterocyclic molecules (Scheme 3).

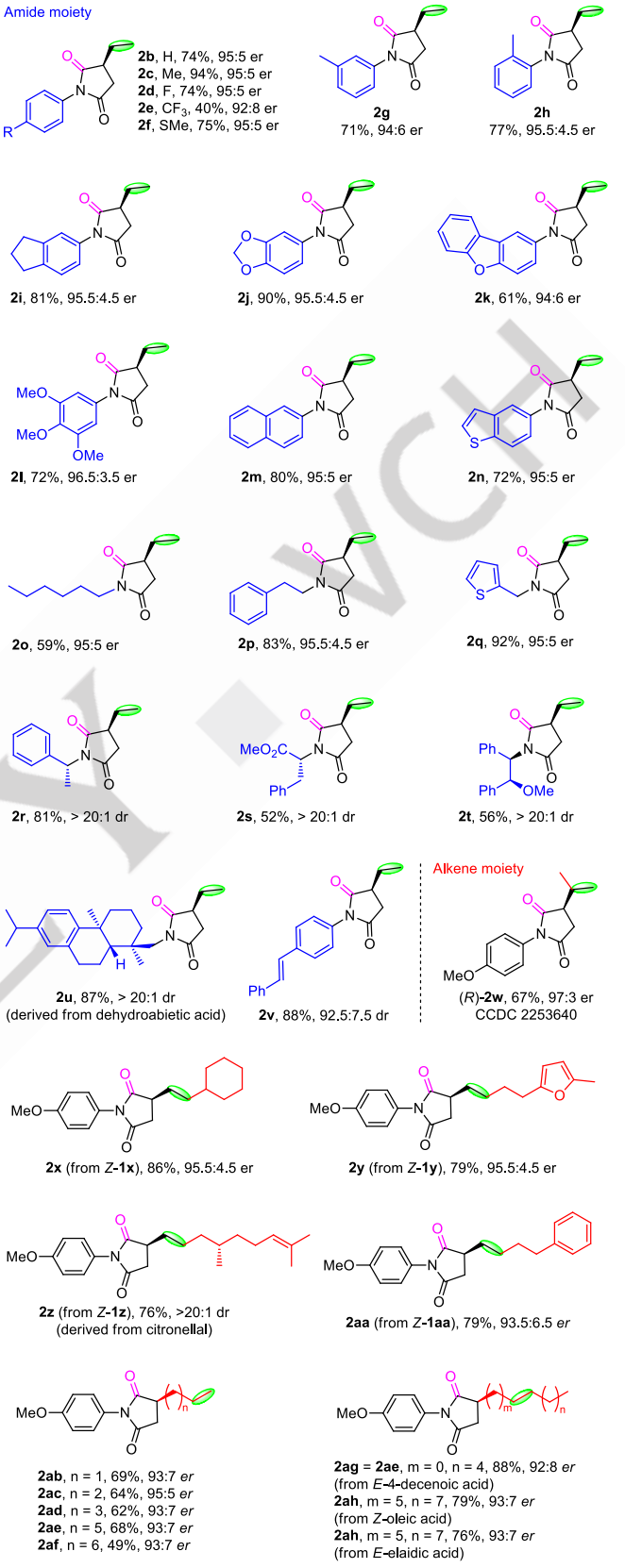

Scheme 1. Scope of enantioselective migratory hydroamidocarbonylation. Reaction conditions: alkene **1** (0.2 mmol), $Pd(OAc)_2$ (2.5 mol%), **L1** (5.6 mg, 3 mol%), PTSA (9.2 mg, 24 mol%), xylenes (1 mL), 30 bar CO, 80 °C, 24 h. Isolated yields. The *er* values were determined by chiral HPLC.

10.1002/anie.202410967

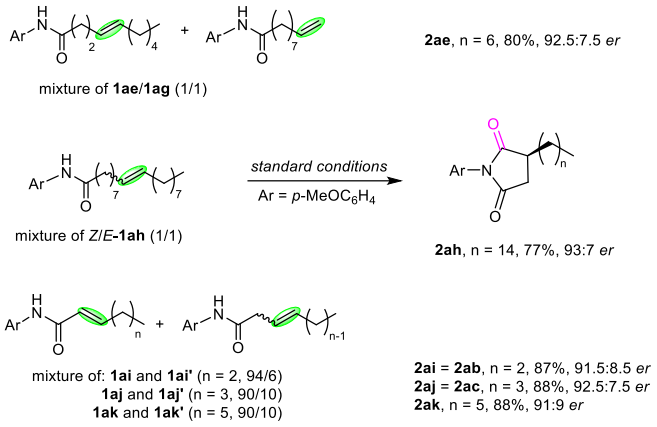

Scheme 2. Regio- or stereo-convergent synthesis from mixture of olefin isomers.

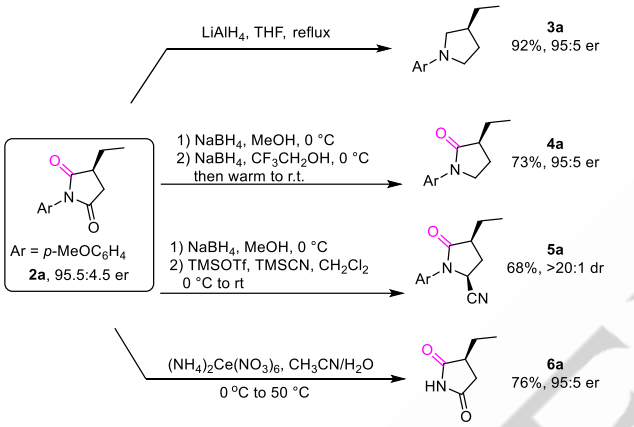

Scheme 3. Transformation of chiral succinimide product.

The apparent differences on the product yield using **L1** and **L3** with different substitution on 4,4'-position of 2,3-dihydrobenzo[*d*][1,3]oxaphosphole skeleton (Table 1, entry 1 *vs.* 3) led us to investigate the reaction kinetics profiles. The compositional variations of substrate, product and intermediates with the reaction process were monitored by gas chromatography (Figure 2). The results showed that the isomerization of terminal alkene **1a** to (*E*)/(*Z*)-mixture of internal alkene intermediate **1a'** proceeded smoothly at the initial stage of reaction. The proportion of **1a'** reached a maximum at 2 h. With the proceeding of hydroamidocarbonylation, **1a'** was gradually converted to chiral product **2a**. During the reaction, thermodynamically more stable α,β-unsaturated amide was not observed. Using **L3** instead of **L1** resulted in a lower yield after 9 h, although **1a** and **1a'** were both consumed up. Further analysis of the reaction mixture with **L3** by high-resolution mass spectrometry revealed that besides **2a**, linear carboxylic acid by hydrocarboxylation, *N*-(4-methoxyphenyl)-4-methylbenzene-sulfonamide by amine exchange, and branched ketone by hydroacylation were detected (Figure S1 in SI). This evidence indicated the lower chemoselectivity towards migratory hydroamidocarbonylation when **L3** was employed to replace **L1**. The comparison between the reaction profiles of **L1** and **L5** disclosed that switching the *P*-substitution of the ligand skeleton from 1-admantyl to *tert*-butyl substitution had little impact on the rate of alkene isomerization or hydroamidocarbonylation (Figure S4 in SI). Further kinetic profiles suggested that applying axially ligand (*R*)-Segphos in the process resulted in poor reactivity and enantioselectivity (65:35 *er*) (Figure S5 in SI).

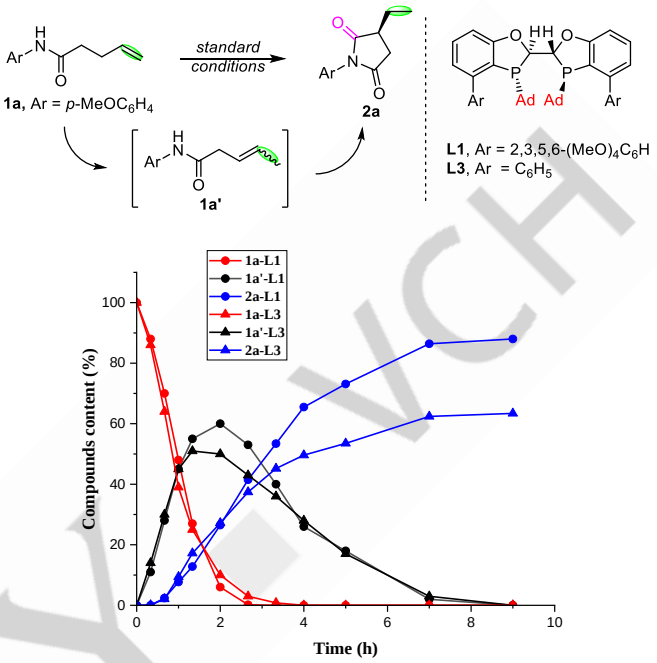

Figure 2. Reaction kinetic profiles of migratory hydroamidocarbonylation of **1a**.

To gain further insight on the isomerization-carbonylation process, the reactivity of acrylamide **1al**, branched terminal alkenes **1am** and **1an**, and thioamide analogue **1ao** was examined under the standard conditions (Figure 3a). The poor conversion of **1al** indicated isomerization of conjugated alkene was more sluggish than that of terminal one. In the meantime, the enantioselectivity was unaffected. The presence of substituent on the carbon chain or replacing amidyl by thioamidyl group totally inhibited the isomerizing reactivity of alkene. Results of experiment with *N*-deuterated alkene and deuterium-labeled acid showed multiple carbon sites along the chain of **2ac** were deuterated (Figure 3b), revealing the involvement of Pd-H species and the reversibility of isomerization process.

According to the reaction kinetic profile, control experiment studies and density functional theory (DFT) calculations, a plausible mechanism was proposed (Scheme 4). The tandem isomerization-hydroamidocarbonylation probably proceeds via the following steps: i) the generation of active Pd-H complex through the oxidation of Pd(0) complex by *p*-toluenesulfonic acid; ii) isomerizing terminal alkene to internal intermediate by Pd-H complex; iii) inserting the internal alkene into the Pd-H bond to generate Pd-alkyl complex; iv) inserting CO into the Pd-alkyl bond; v) Reductive elimination of Pd-acyl complex or nucleophilic attack of Pd^{+}-acyl species by intramolecular amido nitrogen leading to the final product. The results of DFT calculations suggested that the coordination of carbonyl group with Pd(II) center may lead to

10.1002/anie.202410967

the formation of a stable five-membered cyclic Pd-alkyl intermediate, which can inhibit the further β-H elimination to α,β-unsaturated amide (Figure S10 and S11 in SI). With ligand **L6** to compute the energy profile of this reaction, the calculation results revealed the enantioselectivity and catalytic activity are both determined by the step of reductive elimination of Pd-acyl intermediate (Figure S12 in SI).

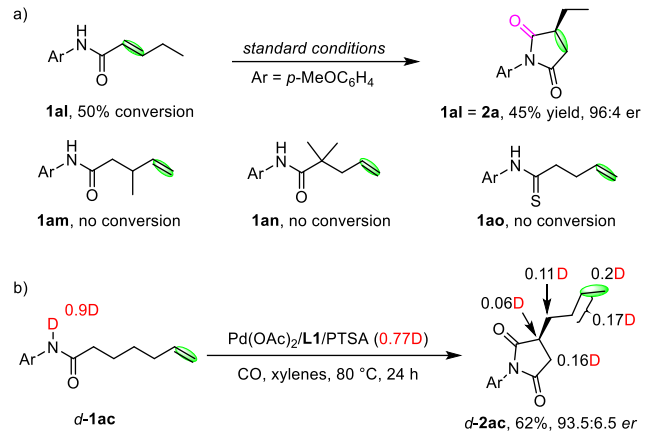

Figure 3. Migratory hydroamidocarbonylation.

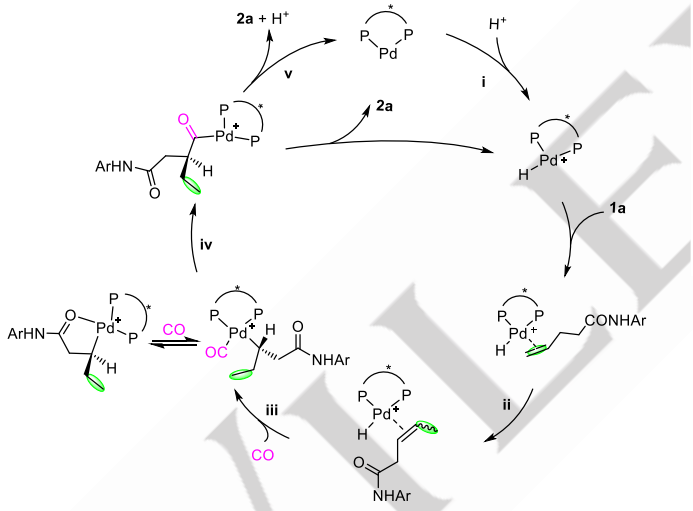

Scheme 4 Proposed reaction mechanism.

The ligand steric effects on enantioselectivity were then evaluated using the topographic steric maps. Generally, the cationic Pd(II)-H complex was regarded as the active catalyst.[22,28] We optimized the structure of chiral cationic Pd(II) carbonyl hydride complexes chelated with **L1**, **L2**, **L3**, **L6**, and (*R*)-Segphos, respectively. By SambVca web application,[36] the topographic steric maps of these palladium complexes were drawn to visualize the steric hinderance around palladium center and the percentage of buried volume (**%V$_{bur}$**) was calculated to quantify the depth of these chiral catalytic pockets (Figure 4). The larger **%V$_{bur}$** indicates the deeper catalytic pocket. The results illustrated that the strong hindrance of **L1** is contributed from the tetra-methoxy-substituted phenyl groups in the northern and southern hemispheres, and truncating the methoxy substitutions on the two phenyl rings leads to significant diminishing of steric hinderance around the palladium center (**L1** *vs.* **L2** and **L3**). Correspondingly, the **%V$_{bur}$** is reduced from 69.7% (**L1**) to 64.0% (**L3**). Changing the *P*-substitutions from bulky 1-adamantly to smaller *tert*-butyl group results to less steric hinderance in the eastern and western hemispheres of chiral catalytic pocket. At the meantime, **%V$_{bur}$** is reduced from 68.1% (**L2**) to 66.9% (**L6**). Compared with these *P*-chiral bidentate phosphine ligands based on geometrically rigid skeleton, the **%V$_{bur}$** of classical axially chiral ligand (*R*)-Segphos is only 54.1%, suggesting significantly shallower chiral catalytic pocket. Noteworthily, the steric hinderance is drastically reduced in the northern and southern hemispheres of its catalytic pocket. These visible changes of the pocket depth and steric hinderance around Pd center resulted from the structural difference of ligand rationalized the observed enantioselectivity with different chiral ligands. The deeper catalytic pocket and the stronger steric hinderance around Pd center created by the rigid 2,3-dihydrobenzo[*d*][1,3]oxaphosphole skeleton and bulky substitutions (i.e., 2,3,5,6-tetramethoxyphenyl and 1-adamantyl groups) are beneficial to achieve higher enantioselectivity.

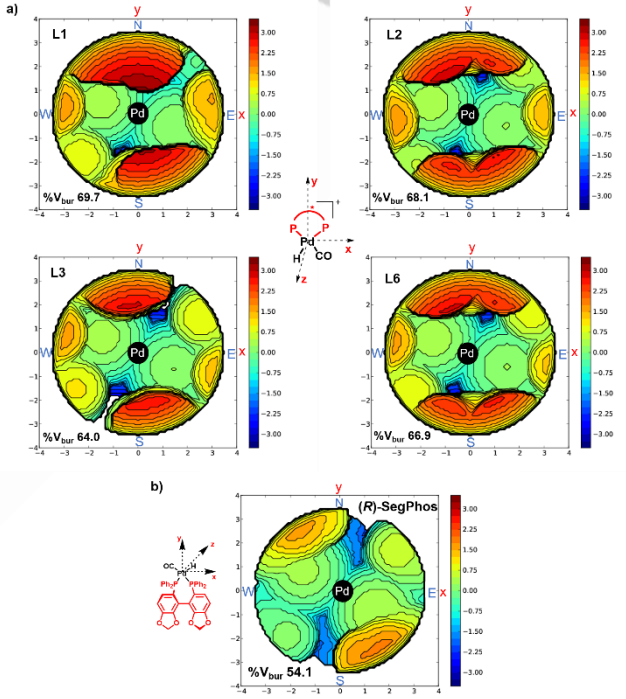

Figure 4. The steric maps based on DFT-optimized structures of five cationic palladium(II) carbonyl hydride complexes chelated with different chiral bisphosphine ligands. Only the red parts of ligands were considered in the definition of the catalytic pocket. The steric maps are viewed down the z-axis; the orientation of the complexes is indicated. The isocontour scheme, in Å, is shown at the right side of each map. The red and blue zones indicate the more- and less-hindered zones in the catalytic pocket, respectively. Comparison of the steric maps allows differences to be identified in the shapes of the catalytic pockets. %**V$_{bur}$** = percentage of buried volume.

Conclusion

A Pd-catalyzed enantioselective migratory hydroamidocarbonylation of terminal and internal alkenes bearing a secondary amide group was developed, affording a variety of chiral α-alkyl succinimides in moderate to good yields with high *er* values. Regio- or stereo-convergent synthesis of enantiomeric

succinimides from the mixture of olefin isomers can be achieved by using this procedure. The combined experimental and theoretical mechanistic studies revealed rigid *P*-chirogenic bisphosphine ligand bearing bulky *P*-adamantyl and 2,3,5,6-tetramethoxyphenyl groups was crucial to the successful reaction, which allows for stronger steric hinderance and deeper catalytic pocket in the key steps.[37]

Acknowledgements

This work was financially supported by the National Key R&D Program of China (2023YFA1507500), the National Nature Science Foundation of China (22271094), Shanghai Rising Star Program (21QA1402800), and the Innovation Program of Shanghai Municipal Education Commission (2023ZKZD37).

Keywords: carbonylation • asymmetric catalysis • isomerization • chiral succinimides • palladium

[1] V. P. Ananikov, M. Tanaka, *Hydrofunctionalization*, Springer, Heidelberg, 2013.

[2] X. Cui, K. Burgess, *Chem. Rev.* **2005**, *105*, 3272.

[3] J. R. Coombs, J. P. Morken, *Angew. Chem. Int. Ed.* **2016**, *55*, 2636; *Angew. Chem.* **2016**, *128*, 2682.

[4] Z. Sorádová, R. Šebesta, *ChemCatChem* **2016**, *8*, 2581.

[5] J. Chen, Z. Lu, *Org. Chem. Front.* **2018**, *5*, 260.

[6] R. Liu, S. L. Buchwald, *Acc. Chem. Res.* **2020**, *53*, 1229

[7] X.-Y. Sun, B.-Y. Yao, B. Xuan, L.-J. Xiao, Q.-L. Zhou, *Chem Catal.* **2022**, *2*, 3140.

[8] Y. He, J. Chen, X. Jiang, S. Zhu, *Chin. J. Chem.* **2022**, *40*, 65.

[9] A. Vasseur, J. Bruffaerts, I. Marek, *Nature Chem.* **2016**, *8*, 209

[10] H. Sommer, F. Juliá-Hernández, R. Martin, I. Marek, *ACS Cent. Sci.* **2018**, *4*, 153.

[11] Y. Li, D. Wu, H.-G. Cheng, G. Yin, *Angew. Chem. Int. Ed.* **2020**, *59*, 7990; *Angew. Chem.* **2020**, *132*, 8066.

[12] (a) Y. Wang, Y. He, S. Zhu, *Acc. Chem. Res.* **2022**, *55*, 3519; (b) X. Chen, Z. Cheng, J. Guo, Z. Lu, *Nat. Commun.* **2018**, *9*, 3939; (c) S. P. Ross, A. A. Rahman, M. S. Sigman, *J. Am. Chem. Soc.* **2020**, 142, 23, 10516; (d)

[13] (a) E. Larionov, H. Li, C. Mazet, *Chem. Commun.* **2014**, *50*, 9816; (b) A. L. Kocen, M. Brookhart, O. Daugulis, *Chem. Commun.* 2017, 53, 10010; (c) R. Matsuura, M. K. Karunananda, M. Liu, N. Nguyen, D. G. Blackmond, K. M. Engle *ACS Catal.* **2021**, 11, 4239; (d) Q. Ge, J. Meng, H. Liu, Z. Yang, Z. Wu, W. Zhang, *Chin. J. Chem.* **2022**, 40, 2269; (e) A. R. Rosales, S. P. Ross, P. Helquist, P.-O. Norrby, M. S. Sigman, O. Wiest, *J. Am. Chem. Soc.* **2020**, 142, 9700

[14] F. Zhou, Y. Zhang, X. Xu, S. Zhu, *Angew. Chem. Int. Ed.* **2019**, *58*, 1754; *Angew. Chem.* **2019**, *131*, 1768.

[15] Y. Zhang, J. Ma, J. Chen, L. Meng, Y. Liang, S. Zhu, *Chem* **2021**, *7*, 3171.

[16] Y. He, J. Ma, H. Song, Y. Zhang, Y. Liang, Y. Wang, S. Zhu, *Nature Commun.* **2022**, *13*, 2471.

[17] R. Yu, S. Rajasekar, X. Fang, *Angew. Chem. Int. Ed.* **2020**, *59*, 21436; *Angew. Chem.* **2020**, *132*, 21620.

[18] X. Jiang, F.-T. Sheng, Y. Zhang, G. Deng, S. Zhu, *J. Am. Chem. Soc.* **2022**, *144*, 21448

[19] J.-W. Wang, Z. Li, D. Liu, J.-Y. Zhang, X. Lu, Y. Fu, *J. Am. Chem. Soc.* **2023**, *145*, 10411.

[20] (a) V. V. Grushin, *Chem. Rev.* **1996**, *96*, 2011; (b) E. Larionov, H. Li, C. Mazet, *Chem. Commun.* **2014**, *50*, 9816; (c) R. Blieck, M. Taillefer, F. Monnier, *Chem. Rev.* **2020**, *120*, 13545; (d) K. S. Yang, J. A. Gurak, Jr., Z. Liu, K. M. Engle, *J. Am. Chem. Soc.* **2016**, *138*, 14705.

[21] (a) Y.-W. Chen, Y. Liu, H.-Y. Lu, G.-Q. Lin, Z.-T. He, *Nature Commun.* **2021**, *12*, 5626; (b) Y.-C. Wang, Z.-X. Xiao, M. Wang, S.-Q. Yang, J.-B. Liu, Z.-T. He, *Angew. Chem. Int. Ed.* **2023**, *62*, e202215568; *Angew. Chem.* **2023**, *135*, e202215568 (c) X.-X. Chen, H. Luo, Y.-W. Chen, Y. Liu, Z.-T. He, *Angew. Chem. Int. Ed.* **2023**, *62*, e202307628; *Angew. Chem.* **2023**, *135*, e202307628; (d) Q.-Y. Liao, C. Ma, Y.-C. Wang, S.-Q. Yang, J.-S. Ma, Z.-T. He, *Chin. Chem. Lett.* **2023**, *34*, 108371.

[22] (a) G. Kiss, *Chem. Rev.* **2001**, *101*, 3435; (b) R. Sang, Y. Hu, R. Razzaq, R. Jackstell, R. Franke, M. Beller, *Org. Chem. Front.* **2021**, *8*, 799; (c) Y.-H. Yao, H.-Y. Yang, M. Chen, F. Wu, X.-X. Xu, Z-H. Guan, *J. Am. Chem. Soc.* **2021**, 143, 1, 85; (d) T. Seidensticker, M. R. L. Furst, R. Frauenlob, J. Vondran, E. Paetzold, U. Kragl, A. J. Vorholt, *ChemCatChem* **2015**, *7*, 4085.

[23] K. Dong, X. Fang, S. Gu, R. Jackstell, M. Beller, *Nature Commun.* **2017**, *8*, 14117.

[24] (a) P. Roesle, C. J. Dürr, H. M. Möller, L. Cavallo, L. Caporaso, S. Mecking, *J. Am. Chem. Soc.* **2012**, *134*, 17696; (b) J. T. Christl, P. Roesle, F. Stempfle, P. Wucher, I. Göttker-Schnetmann, G. Müller, S. Mecking *Chem. Eur. J.* **2013**, *19*, 17131; (c) P. Roesle, L. Caporaso, M. Schnitte, V. Goldbach, L. Cavallo, S. Mecking, *J. Am. Chem. Soc.* **2014**, *136*, 16871; (d) V. Goldbach, L. Falivene, L. Caporaso, L. Cavallo, S. Mecking, *ACS Catal.* **2016**, *6*, 8229.

[25] (a) C. Jimenez Rodriguez, D. F. Foster, G. R. Eastham, D. J. Cole-Hamilton, *Chem. Commun.* **2004**, 1720; C. H. Low, J. D. Nobbs, M. van Meurs, L. P. Stubbs, E. Drent, S. Aitipamula, M. H. L. Pung, *Organometallics* **2015**, *34*, 4281; (b) L. Zhao, B. Pudasaini, A. Genest, J. D. Nobbs, C. H. Low, L. P. Stubbs, M. van Meurs, N. Rösch, *ACS Catal.* **2017**, *7*, 7070; (c) L. Zhao, B. Pudasaini, A. Genest, J. D. Nobbs, C. H. Low, L. P. Stubbs, M. van Meurs, N. Rösch, *ACS Catal.* **2017**, *7*, 7070; (d)J. D. Nobbs, C. H. Low, L. P. Stubbs, C. Wang, E. Drent, M. van Meurs, *Organometallics* **2017**, *36*, 391.

[26] (a) J. Li, Y. Shi, *Chem. Soc. Rev.* **2022**, *51*, 6757; (b) J.-B. Peng, X.-L. Liu, L. Li, X.-F. Wu, *Sci. China Chem.* **2022**, *65*, 441; (c) C. Shen, K. Dong, *Synlett* **2022**, *33*, 815; (d) H. Li, K. Dong, H. Neumann, M. Beller, *Angew. Chem. Int. Ed.* **2015**, 54, 10239-10243; *Angew. Chem.* **2015**, 127, 10377; (e) H.-Y. Yang, Y.-H. Yao, M. Chen, Z.-H. Ren, Z.-H. Guan, *J. Am. Chem. Soc.* **2021**, 143, 7298; (f) H. Li, X. Fang, R. Jackstell, H. Neumann, M. Beller, *Chem. Commun.* **2016**, 52, 7142.

[27] T. C. Jankins, W. C. Bell, Y. Zhang, Z.-Y. Qin, J. S. Chen, M. Gembicky, P. Liu, K. M. Engle, *Nature Chem.* **2022**, *14*, 632.

[28] (a) X. Ren, Z. Wang, C. Shen, X. Tian, L. Tang, X. Ji, K. Dong, *Angew. Chem, Int. Ed.* **2021**, *60*, 17693; *Angew. Chem.* **2021**, *133*, 17834. (b) X. Ji, C. Shen, X. Tian, H. Zhang, X. Ren, K. Dong, *Angew. Chem, Int. Ed.* **2022**, *61*, e202204156; (c) X. Ji, C. Shen, X. Tian, K. Dong, *Org. Lett.* **2021**, *23*, 8645.

[29] (a) L. Wang, M. Chen, P. Zhang, W. Li, J. Zhang, *J. Am. Chem. Soc.* **2018**, *140*, 3467; (b) J. Xu, Y. Song, J. Yang, B. Yang, Z. Su, L. Lin, X. Feng, *Angew. Chem. Int. Ed.* **2023**, *62*, e202217887; 135, *Angew. Chem.* **2023**, *13*, e202217887.

[30] (a) M. Dutartre, J. Bayardon, S. Jugé, *Chem. Soc. Rev.* **2016**, *45*, 5771; (b) G. Xu, C. H. Senanayake, W. Tang, *Acc. Chem. Res.* **2019**, *52*, 1101.

[31] (a) X. Li, J. Jin, P. Chen, G. Liu. *Nature Chem.* **2022**, *14* , 425; (b) X. Li, X. Yang, P. Chen, G. Liu *J. Am. Chem. Soc.* **2022**, *144*, 22877.

[32] G. Liu, X. Liu, Z. Cai, G. Jiao, G. Xu, W. Tang *Angew. Chem. Int. Ed.* **2013**, *52*, 4235.

[33] G. Bettoni, C. Cellucci, F. Berardi, *J. Heterocyclic Chem.* **1980**, *17*, 603.

[34] Deposition Number 2253640 (for **2w**) contains the supplementary crystallographic data for this paper. These data are provided free of charge by the joint Cambridge Crystallographic Data Centre and Fachinformationszentrum Karlsruhe Access Structures service.

[35] A. A. N. Magro, L.-M. Robb, P. J. Pogorzelec, A. M. Z. Slawin, G. R. Eastham, D. J. Cole-Hamilton, *Chem. Sci.* **2010**, 1, 723–730.

[36] L. Falivene, R. Credendino, A. Poater, A. Petta, L. Serra, R. Oliva, V. Scarano, L. Cavallo, *Organometallics* **2016**, 35, 2286; (b) L. Falivene, Z. Cao, A. Petta, L. Serra, A. Poater, R. Oliva, V. Scarano, L. Cavallo, *Nature Chem.* **2019**, 11, 872.

[37] X.-J. Zou, Z.-X. Jin, H.-Y. Yang, F. Wu, Z.-H. Ren, Z.-H. Guan, *Angew. Chem. Int. Ed.* **2024**, e202406226.

10.1002/anie.202410967

WILEY VCH

RESEARCH ARTICLE

Entry for the Table of Contents

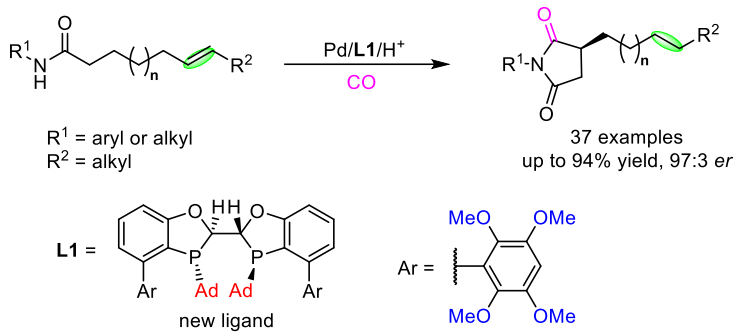

Improve **enantioselectivity** and **activity** by introducing **-Ad** & **-OMe** groups!

A Pd-catalyzed enantioselective isomerization-hydroamidocarbonylation of amide-containing alkenes to access chiral α-alkyl succinimides was developed. The key to success was adopting *P*-chirogenic bisphosphine ligand featured with bulky 1-adamentyl *P*-substitution and 2,3,5,6-tetramethoxyphenyl group to create stronger steric hinderance and deeper catalytic pocket.